

273

MRB4014Q5

UNCLASSIFIED

29p. 0.75

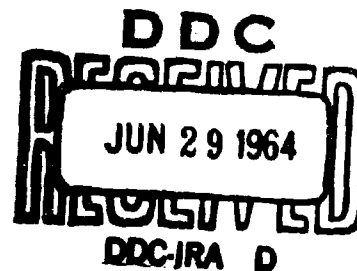
MONSANTO RESEARCH CORPORATION
BOSTON LABORATORY
Everett, Massachusetts, 02149
Contract No. DA18-108-AMC-238 (A)

Fifth Bimonthly Progress Report

Covering the Period
1 March - 30 April 1964

NEW CONCEPT STUDIES, CW DEFENSE

Prepared by
J. O. Smith, B. M. Fabuss, D. A. Duncan, C. H. Lu
15 June 1964



Copy 27 of 26 copies

UNCLASSIFIED

601645

ABSTRACT

Adsorption experiments with GA-agent on activated carbon were completed at 30 and 45°C in the 2-500 microgram per liter concentration range. The data were expressed in the form of Langmuir type adsorption isotherms. The adsorption of GA-agent on activated carbon is less than monomolecular. The effect of water vapor on the adsorbed quantities of GA-agent was found to be negligible up to a 85% relative humidity, a slight reduction of adsorptive capacity of 5-25% occurs at humidities exceeding 85% relative humidity. The desorption rate of adsorbed agent was extremely low.

A simplified method was developed to correlate the experimental data on capillary penetration and retentive capacity of liquids in sorbent beds. A correlation between the sorption rate and capacity was developed. Measurements of the sorption of GF-agent and GB-agents are being conducted.

TABLE OF CONTENTS

| | <u>Page</u> |
|--|-------------|
| I. INTRODUCTION AND SUMMARY. | 1 |
| A. ADSORPTION FROM THE VAPOR PHASE | 1 |
| B. LIQUID SORPTION | 1 |
| II. ADSORPTION OF GA-AGENT FROM VAPOR PHASE | 1 |
| A. THE 30°C ADSORPTION ISOTHERM. | 1 |
| B. 45°C ADSORPTION ISOTHERM DATA | 5 |
| C. CHARACTER OF ADSORPTION | 7 |
| D. THE EFFECT OF WATER HUMIDITY. | 10 |
| E. DESORPTION BY DRY NITROGEN. | 13 |
| F. BREAKTHROUGH CURVES | 14 |
| III. LIQUID PHASE SORPTION | 14 |
| A. CAPILLARY PENETRATION | 14 |
| B. RETENTIVE CAPACITY. | 15 |
| C. CORRELATION OF CAPILLARY PENETRATION AND RETENTIVE CAPACITY. | 20 |
| D. MEASUREMENTS ON CHEMICAL WARFARE AGENTS | 24 |
| IV. REFERENCES. | 24 |

LIST OF TABLES

| <u>Number</u> | | <u>Page</u> |
|---------------|--|-------------|
| 1 | ADSORPTION OF GA-AGENT ON ACTIVATED CARBON - ISO-THERM DATA. | 2 |
| 2 | ADSORPTION OF GA-AGENT ON ACTIVATED CARBON - EFFECT OF WATER VAPOR. | 11 |
| 3 | INTERCEPTS AND SLOPE CONSTANTS. HORIZONTAL CAPILLARY PENETRATION THROUGH POROUS BEDS OF RANDOM-PACKED PARTICLES. | 16 |
| 4 | RETENTIVE CAPACITIES OF SOME SOLID SORBENTS | 18 |
| 5 | DEPTH OF CAPILLARY PENETRATION OF BENZENE AND THE VOLUME RETAINED BY RANDOM-PACKED POROUS BEDS. | 21 |

LIST OF FIGURES

| <u>Number</u> | | <u>Page</u> |
|---------------|---|-------------|
| 1 | Reduced Langmuir plot of GA-agent Adsorption. | 6 |
| 2a | Model of GA-Agent Molecule. Groups Fully Extended, Maximum Area. | 9 |
| 2b | Model of GA-Agent Molecule Groups Tightly Packed, Minimum Area. | 9 |
| 3 | Effect of Water Vapor on GA Adsorption, Run No. GA 0430 | 12 |
| 4 | Correlation of Experimental Data on Horizontal Capil- lary Penetration of Liquids Through Random Packed Porous Beds | 17 |
| 5 | Correlation of Experimental Data on Retentive Capacity of Random-Packed Porous Beds. | 19 |
| 6 | Depth of Horizontal Capillary Penetration of Benzene Through Random-Packed Porous Beds | 22 |
| 7 | Volume of Benzene Retained by Random-Packed Porous Beds as a Function of Contact Time. | 23 |

I. INTRODUCTION AND SUMMARY

A. ADSORPTION FROM THE VAPOR PHASE

Experimental work to define the adsorption isotherm at 30°C for GA-agent on activated carbon was completed. Even at GA-agent concentrations as low as 2 gamma per liter adsorption capacities of the order of one-half gram of GA-agent per gram of carbon were observed. Only a slight trend in adsorption capacity was found over the GA-agent concentration range studied (2-500 gamma per liter). The average value for adsorption capacity was 571 mg per gram of carbon.

The same, almost insignificant trend characterized the isotherm data at 45°C. The average adsorption value at this temperature was 517 mg of GA-agent per gram of carbon.

Water vapor from a humid carrier gas was co-adsorbed with GA-agent on the activated carbon only very slightly. At the 85% water saturation level about 5% of the adsorption capacity of the carbon was taken up by the water.

Desorption of GA from a saturated carbon adsorbent by a dry nitrogen stream proceeded very slowly. Under the usual experimental conditions of this work the desorption rate was one-half milligram per hour.

B. LIQUID SORPTION

In sorption of liquids on sorbents, a new correction factor was obtained in correlating experimental data on capillary penetration and retentive capacity. This factor was a function of porosity only and can be used directly in the correlation equations. The introduction of this correction factor will simplify the calculation considerably.

A correlation was established between the capillary penetration and retentive capacity. The amount of liquid retained by the porous bed as a function of contact time can be estimated from the experimental data from these two studies.

II. ADSORPTION OF GA-AGENT FROM VAPOR PHASE

A. THE 30°C ADSORPTION ISOTHERM

The data reported in the last progress report (ref. 1) on adsorption of GA-agent on Pittsburgh Chemical Company activated carbon (30 x 40 mesh, Type BPL) at 30°C have been extended to both lower and higher GA-agent concentrations. The same experimental method described in that report was used in this recent work. The results from the new 30°C isotherm runs and three runs at 45°C are listed in Table 1.

Table 1

ADSORPTION OF GA-AGENT ON ACTIVATED CARBON-ISOTHERM DATA

Carbon: Pittsburgh Chemical Company, Type BPL -30 + 40 Mesh
 Bed Size: 200 mg, 5.95 mm diameter

| <u>Run No.</u> | <u>Volume Flow Rate, liters hr</u> | <u>Water Saturation, %</u> | <u>GA Conc., gamma liter</u> | <u>GA Wt. Flow Rate, mg hr</u> | <u>Carrier Gas</u> | <u>Adsorption Temperature, °C</u> | <u>Break- through Time, min.</u> | <u>Ads Cap Cal mg g</u> |
|----------------|--|------------------------------------|--|--|------------------------|---|--|---|
| 206 | 154 | 38.9 | 305 | 46.9 | air | 30 | 58 | |
| 221 | 154 | 38.9 | 467 | 41.9 | air | 30 | 85.3 | |
| 304 | 160 | 0 | 121 | 19.4 | N ₂ | 30 | 265 | |
| 305 | 160 | 0 | 59.7 | 9.58 | N ₂ | 30 | 569 | |
| 310 | 154 | 0 | 55.4 | 8.5 | N ₂ | 30 | -- | |
| 306 | 137 | 0 | 9.6 | 1.38 | N ₂ | 30 | 38.0 | |
| 314 | 135 | 0 | 2.07 | 0.27 | N ₂ | 30 | 9.5 days | |
| 413 | 159 | 0 | 260 | 41.3 | N ₂ | 45 | 131 | |
| 415 | 163 | 0 | 234 | 38.1 | N ₂ | 45 | 120 | |
| 417 | 144 | 0 | 29.5 | 4.3 | N ₂ | 45 | -- | |

CARBON-ISOTHERM DATA

Type BPL -30 + 40 Mesh

| Adsorption Temperature, °C | Break- through Time, min. | Adsorption Capacity Calculated, <u>mg QA</u> <u>g C</u> | Adsorption Capacity by Wt. <u>mg QA</u> <u>g C</u> |
|----------------------------------|------------------------------------|---|--|
| 30 | 58 | 520 | -- |
| 30 | 85.3 | 591 | -- |
| 30 | 265 | 511 | 625 |
| 30 | 569 | 517 | 550 |
| 30 | -- | -- | 525 |
| 30 | 38.0 | -- | 250 |
| 30 | 9.5 days | -- | 475 |
| 45 | 131 | -- | 525 |
| 45 | 120 | 460 | 525 |
| 45 | -- | -- | 500 |

Although no difference in adsorption capacity has been detected whether air or nitrogen is used as the carrier gas, nitrogen has been used for most of this isotherm work so that the isotherms could be defined free from possible oxidation effects. In the low GA-agent concentration runs that require a long period of time, effect of oxidation might be appreciable. In all such runs nitrogen has been used.

Because dry nitrogen (no water humidification) was used as the carrier gas for these isotherm runs, it was possible to determine the equilibrium adsorption capacity of the activated carbon for GA-agent by weighing the carbon before and after the adsorption. Where a successful concentration versus time curve was recorded by the flame ionization detector, it was possible to check the value of the adsorption capacity calculated from the concentration curve against that obtained gravimetrically. The check was only fair but was within the expected precision for these data (see Table 1). The calculated adsorption capacity values were lower in each case than those obtained by weight. The reason for this is now known.

The GA-agent concentrations used in this experimental work ranged from a high 467 gamma per liter to a low of 2.07 gamma per liter. This low concentration run required 9.5 days for break-through of the agent through the 200-mg bed used.

To completely define the adsorption isotherm of GA-agent on this activated carbon would require experimenting at concentrations below 2 micrograms per liter. This would not only be difficult and time-consuming but also would be more of academic interest than of practical use. The important fact is that this Pittsburgh Chemical Company Type BPL activated carbon has been shown to have high absorptivity for GA-agent over the very wide concentrations range of this study. This means that the protection afforded by this carbon from GA-agent contamination is good from saturated conditions down to concentrations as low as 2 micrograms per liter.

Run number 304 of Table 1 has been reported previously but is included here because the adsorption capacity was determined gravimetrically as well as by concentration-time curve. The adsorption capacities obtained by weighing should certainly be the more accurate of the two sets of values. And, since only a minute trend of adsorption capacity with GA-agent concentration was observed, the best value for the GA-agent capacity of activated carbon is considered to be the average of all the capacities determined by weighing. This value is 571 mg of GA-agent per gram of carbon.

The only exception to the above averaging treatment was the exclusion of the 475 mg/gram value of the 2.07 gamma per liter run. This adsorption capacity value was lower than all others (high 625, low 525) and it was felt that this may be a significant difference because of the low GA-agent concentration.

The data of the measurements presented in Table 1 were evaluated according to a Langmuir type isotherm. The Langmuir isotherm can be given as

$$\frac{p/p_o}{v} = \frac{1}{cv_m} + \frac{p/p_o}{v_m} \quad (1)$$

where, p is the partial pressure of the agent
 p_o is the vapor pressure of the agent
 v is the adsorbed volume of agent
 v_m is the volume of a monomolecular layer
 c is a constant

Also, $\frac{p}{p_o} = \frac{C}{C_o}$

and $C_o = 857.4 \mu\text{g/l}$

and $v = a/d$

where a is the adsorbed weight, g agent per g adsorbent
 d is the agent density (1.07).

In Table 1 the concentration (C) is expressed in micrograms per liter and the adsorbed weight (a) in grams of agent per gram of carbon. From the experimental points:

$$\frac{C}{a} = 3.997 + 1.744C \quad (2)$$

or
$$a = \frac{C}{3.997 + 1.744C} \quad (3)$$

Equation (2) can be given as

$$\frac{C/C_o}{vd} = \frac{3.997}{C_o} + 1.744 \frac{C}{C_o}$$

or
$$\frac{p/p_o}{v} = \frac{3.997d}{C_o} + 1.744d (p/p_o)$$

$$\frac{p/p_o}{v} = 4.988 \times 10^{-3} + 1.866 p/p_o \quad (4)$$

Comparing equation (1) and (4)

$$\frac{1}{v_m} = 1.866 \text{ and } v_m = 0.536 \text{ cc/g}$$

and
$$C = \frac{1}{v_m \times 4.988 \times 10^{-3}} = 374$$

The experimental data are shown in Figure 1 as a reduced Langmuir isotherm, plotted as c/a versus C . The straight line corresponds to equation (2).

Equation (3) can also be expressed in the usual form of a Langmuir isotherm:

$$a_g = \frac{0.2502 \times 10^9 [GA]}{1 + 0.4363 \times 10^9 [GA]} \quad (5)$$

where a_g is the adsorbed quantity in g/g
 $[GA]$ is the concentration in g/ml

or changing to g/ml units by multiplying by the bulk density of the adsorbent (0.368 g/ml):

$$a_v = \frac{9.207 \times 10^7 [GA]}{1 + 4.363 \times 10^8 [GA]} \quad (6)$$

where a_v and $[GA]$ are expressed in g/ml.

B. 45°C ADSORPTION ISOTHERM DATA

Three runs were made with the adsorption temperature set at 45°C to see how the adsorption capacities of GA-agent on activated carbon at this temperature compared with those obtained at 30°C.

These values are also included in Table 1. The two high-concentration runs (234 and 260 gamma per liter) resulted in adsorption capacities of 525 mg/g in each case, while the 29.5 gamma per liter run resulted in a value of 500 mg/g. This is a very small difference and just as at 30°C, the shape of the adsorption isotherm is flat over the concentration range studied. That is, there is no significant change in adsorption capacity with changing GA-agent concentration.

The average value of the adsorption capacity of GA-agent on activated carbon at 45°C is 517 mg/g. Comparing this with the 571 mg/g value at 30°C, the drop in adsorption capacity for the 15°C temperature rise was 9.5% or 0.634% per °C.

The data points determined at 45°C are also included in Figure 1. The equation of the resulting adsorption isotherm

$$\frac{C}{a} = 3.179 + 1.892C \quad (7)$$

Although it was already mentioned that the temperature range investigated was very narrow and the precision of the data was limited, an attempt was made to calculate the isotheric heat of adsorption. From equation (2) and (7) at a value of $a_g = 0.5$, on the flat portion of the isotherm:

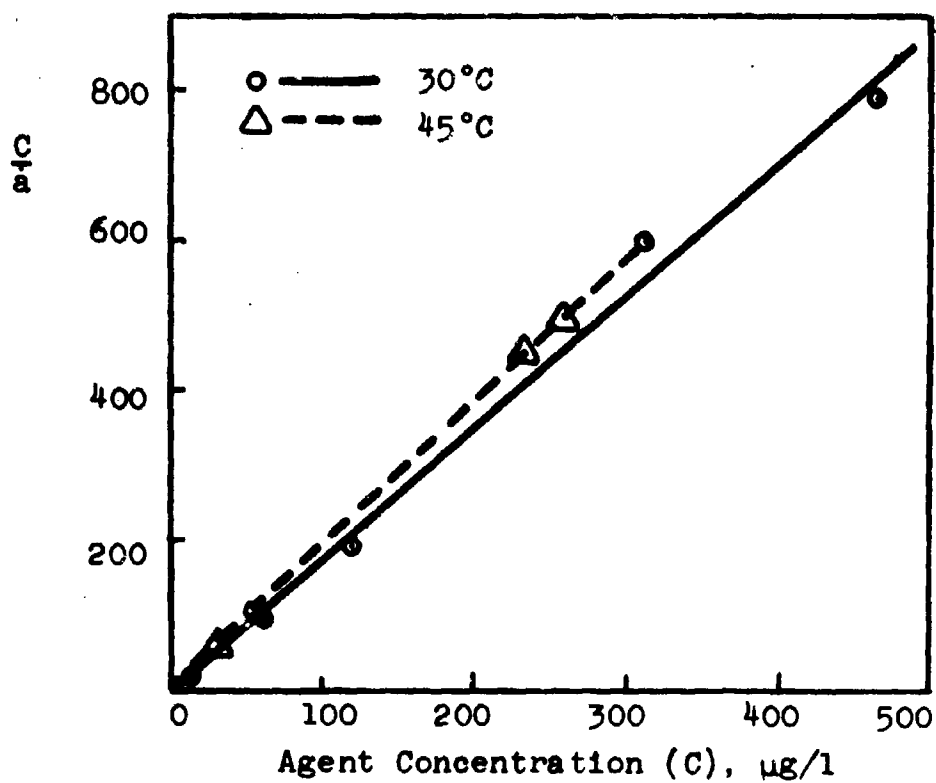


Figure 1. Reduced Langmuir plot of GA-agent adsorption.

$$C_{30^{\circ}\text{C}} = 15.61 \text{ } \mu\text{g/l}$$

$$C_{45^{\circ}\text{C}} = 29.44 \text{ } \mu\text{g/l}$$

and

$$q = \frac{RT_1 T_2}{T_1 - T_2} \log_e \frac{p_1}{p_2} = \frac{1.986 \times 318 \times 303}{318 - 303} \times 2.303 \log \frac{29.44}{15.61} =$$

$$8.095 \text{ cal/mole}$$

(8)

For comparison the heat of vaporization of GA-agent calculated from the vapor pressure data is 13.100 cal/mole. The magnitude of these numbers indicates only the purely physical nature of the adsorption process.

The drop in adsorption capacity as the adsorption temperature was raised agrees with theory and experience. The flat isotherm confirms our experience at 30°C. No further isotherm work is proposed for the immediate future.

C. CHARACTER OF ADSORPTION

In our previous report it was assumed, that the pore volume of the adsorbent, given by the manufacturer as 0.8 cc/g carbon, was filled with condensed GA-agent. If the pores are entirely filled, the adsorption capacity will be $a_g = 0.8 \times 1.07 = 0.856 \text{ g agent/g carbon}$ where 1.07 is the density of GA-agent.

Assuming now that the packing of the molecules on the adsorbent surface approximates that of the liquid agent, the area covered by a single molecule is:

$$a_L = 4 \times 0.866 \left(\frac{M}{4.2 N d_L} \right)^{2/3} \quad (9)$$

where

M = molecular weight

N = Avogadro's number

d_L = density of the liquid

Substituting into equation (7) gives

$$\begin{aligned} a_L &= 4 \times 0.866 \left(\frac{162.1}{4 \times 1.414 \times 6.023 \times 10^{23} \times 1.07} \right) = \\ &= 3.464 \times 1.255 \times 10^{-15} = \\ &= 4.347 \times 10^{-15} \text{ cm}^2 = \\ &= 43.47 \text{ } \text{\AA}^2 \end{aligned}$$

The total surface area of the adsorbent is given as 1050-1150 m²/g, or an average of 1100 m²/g. The required agent weight is:

$$W = a_G = \frac{11 \times 10^6}{4.347 \times 10^{-15} \times 6.023 \times 10^{23}} \times 162.1 = 0.681 \text{ g/g}$$

Finally, from the Langmuir isotherm given by equation (4):

$$v_m = 0.536 \text{ ml/g and } a_G = 0.536 \times 1.07 = 0.573 \text{ g/g}$$

The three values are:

- 0.856 g/g for total filling of pores
- 0.681 g/g for monomolecular coverage of surface area determined and accessible for N₂ adsorption
- 0.573 g/g for monomolecular coverage by GA-agent.

This means that the pores of an average diameter of 20Å are not filled entirely by liquid agent, and they cannot accomodate even a complete monomolecular layer of GA-agent on their entire surface. Assuming that the previously calculated surface area of 43.47Å² covered by one liquid molecule is circular, the average length of a molecule is about 7.4 Å. This corresponds roughly to the molecular dimensions of the GA-agent molecule, which, depending on rotation around the bonds, and on the angle of view, vary between 4 and 10Å.

A model of the GA-agent molecule was made using a Fisher, Hirochfelder and Taylor atom model kit. Two scale drawings of the model are shown in Figure 2. These are plan views looking down on the model as it might be attached to the carbon surface. The drawings were made from photographs of the model.

In Figure 2(a) the molecule is shown fully extended to illustrate its parts and to depict the maximum area that would be taken up on the adsorbent surface. It is assumed that the hydrocarbon part of the molecule would be attached to the hydrophobic or nonpolar carbon surface. Therefore, in both cases illustrated, the hydrocarbon groups are shown on the bottom of these plan views. In Figure 2(b) the hydrocarbon groups have been drawn up in close association with each other since a mutual attraction may exist. This case also serves to illustrate the smallest area demand on the adsorbent. The areas occupied by these molecular configurations were 54.8 and 41.5 Å², respectively. This information supports the foregoing calculations and conclusions on monomolecular coverage since the idealized molecular area was 43.47 Å².

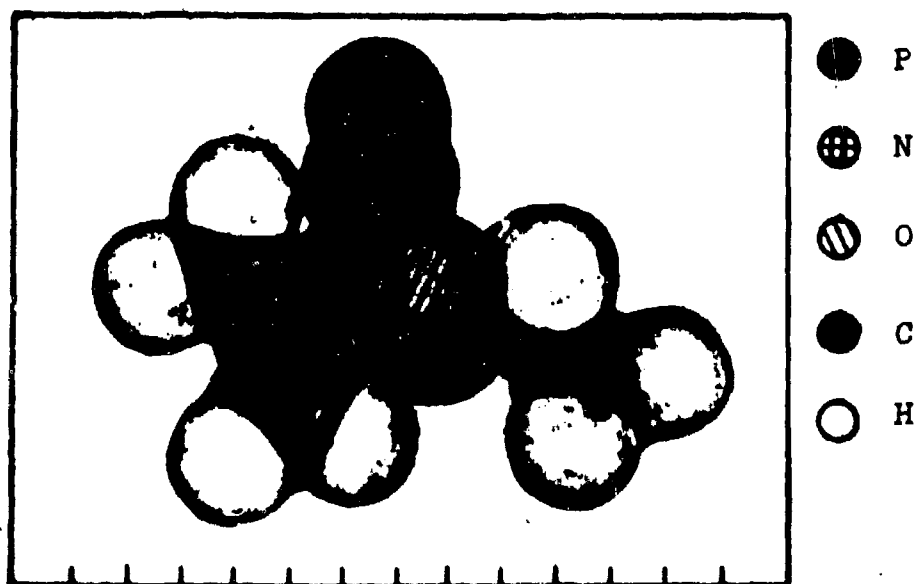


Figure 2a. Model of GA-Agent Molecule.
Groups Fully Extended.
Maximum area.

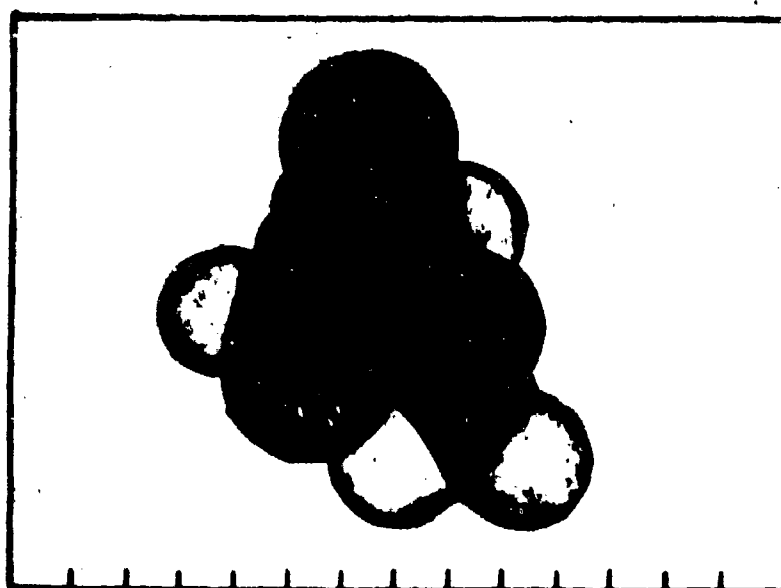


Figure 2b. Model of GA-Agent Molecule.
Groups Tightly Packed.
Minimum Area.

D. THE EFFECT OF WATER HUMIDITY

When the adsorption of HCN on activated carbon was being studied, at the onset of this project it was inadvertently observed that the water vapor added to the air carrier stream had a very significant effect on the extent of the HCN adsorption. The water and HCN molecules were in fact competing for the adsorption sites on the carbon. If water was added, HCN was desorbed and vice versa.

With GA-agent and water vapor the competition for adsorption on the carbon is very much in favor of the GA-agent, so much so that the adsorption-desorption phenomena described for the HCN-water system was never observed with GA-agent and water vapor until the whole flow system had been specially cleaned to enable us to observe this very small effect.

Apparently, even with heated and insulated glass lines, a gradual build-up of GA-agent occurs within the flow system. This results sluggish detection of GA-agent concentration changes and error in calculating the adsorption capacity from the concentration versus time record. Because of this effect, some adsorption capacities were reported in Tables 1 and 2 on a weight basis only; the concentration-time curve was not entirely reliable.

To assure a completely clean system, the flow lines were washed out with acetone and dried overnight with dry nitrogen. Immediately after this procedure run number 430 was made and for the first time, the effect of adding and removing water vapor from the flow stream could be followed by concentration changes recorded by the flame detector.

A diagram of the recorder output of this run, approximately to scale, is given as Figure 3. The pertinent data from this run together with all the "water vapor effect" runs are shown in Table 2.

In run 430 the water saturation was 85.5% and the GA-agent concentration was 251 micrograms/liter. In step 1 the normal adsorption under these conditions took place; 119 mg of GA-agent was adsorbed by the 200 mg bed of -30 + 40 mesh carbon. In step 2 the water vapor was eliminated and an additional 6.29 mg of GA-agent was adsorbed on the carbon. In step 3 the original water vapor concentration was re-established in the flow stream. Here, 2.43 mg of GA-agent was removed from the bed.

The additional GA-agent adsorption caused by removing the water vapor was 5.28% of the original adsorbed or 31.5 mg/gram. However, only 38.7% of the added GA-agent was removed by once again saturating the carrier gas with water vapor to the 85.5% level.

Table 2

ADSORPTION OF GA-AGENT ON ACTIVATED CARBON - EFFECT OF WATER VAPOR

Carbon: Pittsburgh Chemical Co., Type BPL -30 + 40 Mesh
 Bed Size: 200 mg, 5.95 mm diameter

| Run | Water Saturation % | Volume Flow Rate liters/hr | GA Concentration $\frac{\text{gamma}}{\text{liter}}$ | GA Weight Flow Rate $\frac{\text{mg}}{\text{hr}}$ | Carrier Gas | Adsorption Temperature °C | Break through Time min |
|-------|--------------------|----------------------------|--|---|----------------|---------------------------|------------------------|
| 406 | 0 | 112 | 416 | 46.6 | air | 30 | 126 |
| 407-1 | 0 | 110 | 432 | 47.5 | air | 30 | -- |
| 407-2 | 51.2 | 114 | 463 | 52.8 | air | 30 | -- |
| 410 | 51.0 | 135 | 200 | 27.0 | air | 30 | 195 |
| 401 | 68.7 | 110 | 517 | 57.0 | air | 30 | -- |
| 403 | 68.7 | 110 | 430 | 47.0 | air | 30 | 112 |
| 416 | 85.5 | 138 | 123 | 17.1 | N ₂ | 30 | 370 |
| 430 | 85.5 | 116 | 251 | 29.1 | N ₂ | 30 | 228 |
| 423 | 100 | 112 | 271 | 30.4 | N ₂ | 30 | 147 |

* Adsorption Capacity by Wt includes any co-absorbed water

Table 2

ON ACTIVATED CARBON - EFFECT OF WATER VAPOR

Calco Chemical Co., Type BPL -30 + 40 Mesh
5 mm diameter

| GA Weight Flow Rate <u>mg</u> <u>hr</u> | Carrier Gas | Adsorption Temperature <u>°C</u> | Break- through Time <u>min</u> | Adsorption Capacity Calculated <u>mg GA</u> <u>g C</u> | Adsorption Capacity by Wt <u>mg GA</u> <u>g C</u> |
|--|----------------|--|---|--|---|
| 46.6 | air | 30 | 126 | 617 | 550 |
| 47.5 | air | 30 | -- | -- | 625 |
| 52.8 | air | 30 | -- | -- | 650 |
| 27.0 | air | 30 | 195 | 630 | 600 |
| 57.0 | air | 30 | -- | -- | 625 |
| 47.0 | air | 30 | 112 | 558 | 625 |
| 17.1 | N ₂ | 30 | 370 | 475 | 525 |
| 29.1 | N ₂ | 30 | 228 | 595 | -- |
| 30.4 | N ₂ | 30 | 147 | 420 | too wet |

adsorbed water

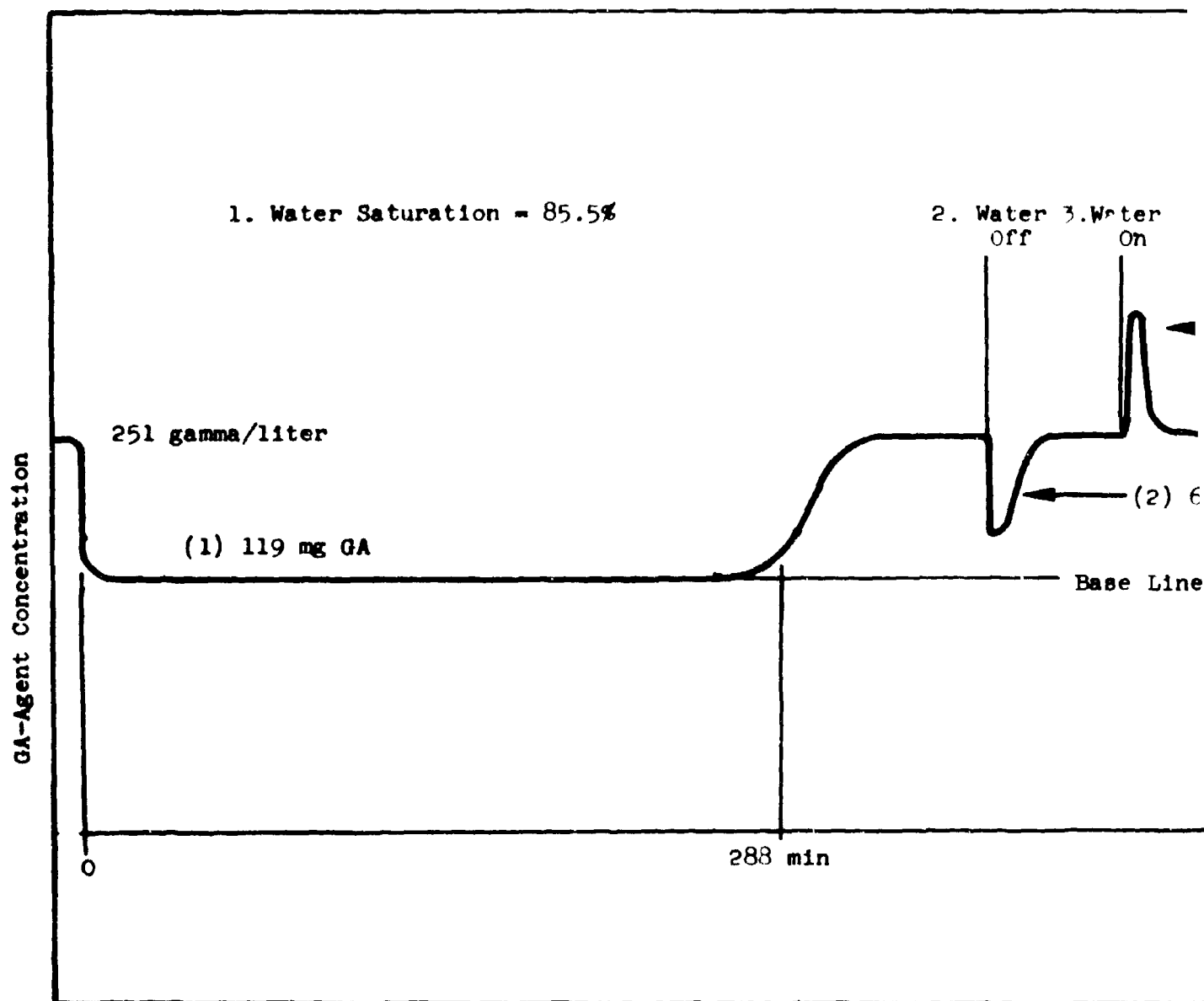
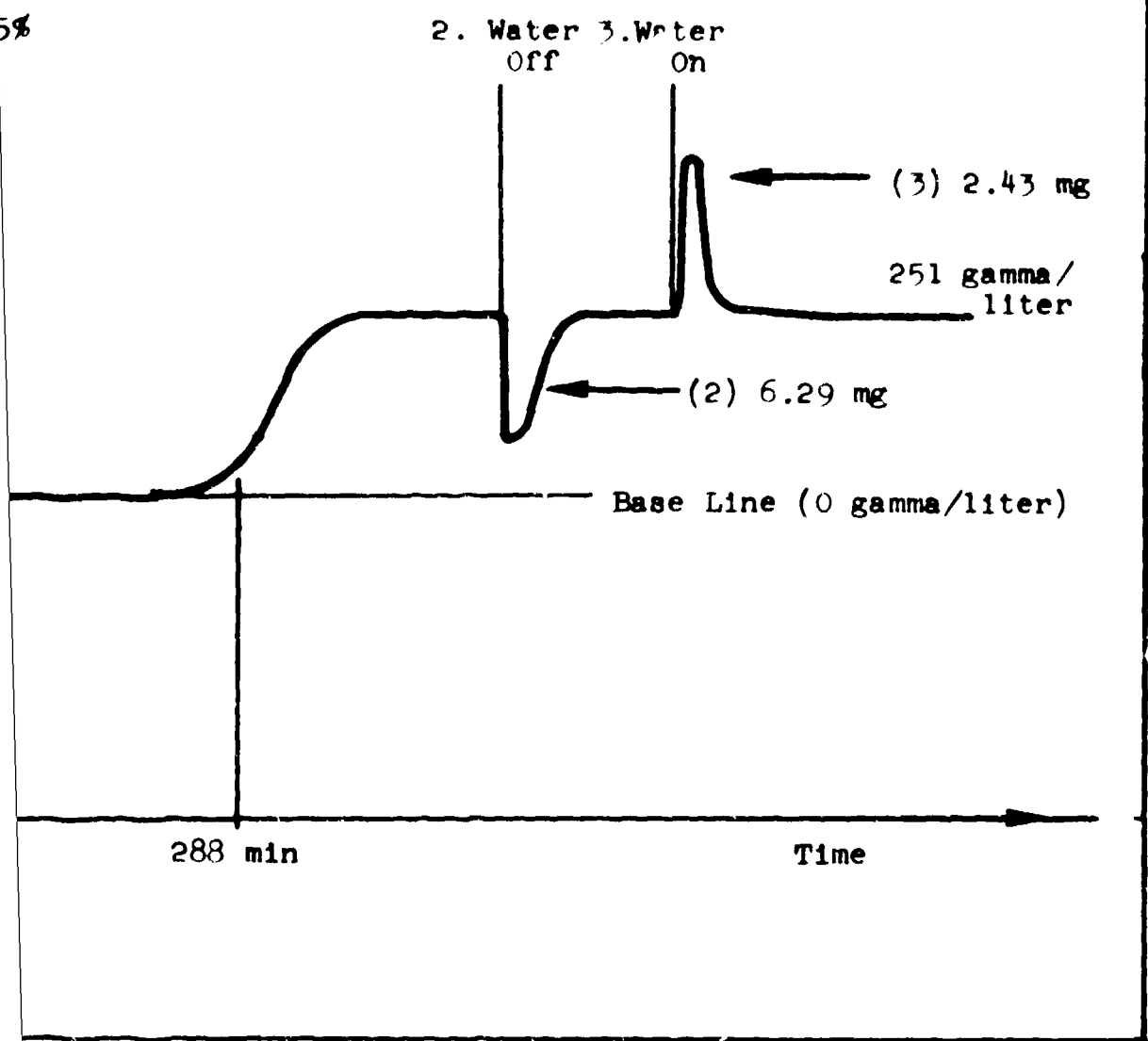


Figure 3. Effect of Water Vapor on GA Adsorption, Run No. GA 0430

58



on GA Adsorption, Run No. GA 0430

Two explanations for the discrepancy in adsorbed and desorbed amounts may be:

- (1) A hysteresis effect, or, more likely,
- (2) The complete desorption is a very slow process. The rate of desorption slows down to below the detectable limit and only the fast initial phase was recorded.

While the effect of the water vapor was slight at this 85.5% saturation level, it could not be detected at lower levels, as expected. For example, in run number 407-1 after the initial absorption was completed with no water vapor in the flow stream, the adsorption bed was weighed. The bed was then allowed to equilibrate with the same GA-agent concentration as before but with a water saturation of 51%. The bed was reweighed and no weight change was observed. While no desorption of GA-agent from the bed by the water was recorded, this doubtless occurred even if only very slightly. The loss in weight due to loss of GA-agent would be made up roughly by the addition of water to the bed.

In run number A23 an attempt was made to establish a water vapor saturation at the adsorber conditions in the vicinity of 95%. The concentration versus time curve indicated a normal run. However, when the carbon was removed for weighing after the adsorption, it was found to be wet with water indicating that the adsorption had proceeded close to or at the 100% saturation level. The calculated adsorption capacity was 420 mg/g, a significantly lower-than-average figure.

It can be concluded that the effect of water vapor in the gas mixture flowing through an adsorber bed is to reduce the amount of GA-agent adsorbed on the activated carbon. The effect is negligible at a water saturation of 50%. At 85% saturation, the adsorption capacity of the bed is reduced by 5%. At 100% saturation it may be as high as 25% but this latter figure is speculative, based on only one run.

B. DESORPTION BY DRY NITROGEN

After the water desorption studies of run 43C were complete (see Figure 2) and the carbon bed was re-established in equilibrium with the water vapor - GA-agent - nitrogen mixture, the water vapor and the GA-agent were both cut off, leaving the bed to be slowly desorbed over a weekend by the dry nitrogen stream.

As might be predicted from the adsorption isotherm data, the desorption rate was very slow. After 65 hours of desorption only 34 mg of GA-agent was removed, or 0.523 mg/hour.

This means that GA-agent leakage from a protective adsorbent layer under field conditions would be very slight even under the influence of a strong wind. Regeneration of a filtering system contaminated with GA-agent would be a tedious procedure, however. The use of heat and lowered pressure could speed up the process.

F. BREAKTHROUGH CURVES

A method of predicting breakthrough capacity and shape of breakthrough curves was outlined in our previous report. Since all our experimental work was carried out on GA-agent of very low volatility and therefore on small adsorber beds, the precision of data is limited and does not permit the development of a more exact predicting method.

A continuation of the research with GB-agent will yield more precise measurements and eliminate any uncertainties connected with the random packing of the presently used small beds. Based on these results the data of our preliminary calculations and estimating methods will be confirmed and extended towards beds where the mass transfer zone is shorter than the length of the total bed of adsorbent (for thin adsorbent layers used in protective clothing).

III. LIQUID PHASE SORPTION

A. CAPILLARY PENETRATION

In the study of horizontal capillary penetration, a "friction-factor factor" and a "Reynolds number factor" were previously introduced in correlating the experimental data (refs. 1 and 2). These factors are available in the literature (ref. 3) as a function of porosity and sphericity. The porosity of the bed can be calculated from the volume of the bed, the weight of the solid, and the particle density of the solid. But the sphericity of the particle can only be estimated from published data (ref. 3). To simplify the calculation procedure and to better represent the data, a new correction factor has been established based on the experimental data from more than 60 runs. This factor is defined as:

$$\text{correction factor} = \frac{X}{(1-X)^2} \quad (10)$$

where X = interstitial porosity, %

It is a function of porosity only and can be used directly in the correlation equations.

Introducing this correction factor, the relationship of experimental variables has the following form:

$$\left[\frac{D_p^2 \gamma_L \cos \theta g_{cp} X}{L \mu^2 (1-X)^2} \right] = a \left[\frac{D_p^2 \rho}{t \mu} \right]^b \quad (11)$$

The notation was given in previous reports (refs. 1 and 2).

Table 3 lists the constants a and b in Equation (11) for five different solids. Of these five, activated carbon, molecular sieve, and silica were studied before, and only the a and b constants for these have been changed according to the new correlation. Silica gel and glass beads are the materials studied during this period. Glass beads are used for the penetration study because they have a definite spherical shape and can be cleaned easily. They are included here to check the validity of the correlation. The zero-degree contact angle lines for the five solids studied are presented in Figure 4.

B. RETENTIVE CAPACITY

More data were obtained on the retentive capacity of solid sorbents. In correlating the experimental data, the same correction factor, $X/(1-X)^2$, used in the penetration study was applied. The experimental variables have the following relationship for gravity draining:

$$\left[\frac{V_L}{V_{BX}} \right] = \phi \left[\frac{D_p^2 \rho g X}{\gamma_L \cos \theta (1-X)^2} \right] \quad (12)$$

The notation was given in the previous report (ref. 2).

The retentive capacities for activated carbon, silica gel, molecular sieve, and silica are presented in Table 4 and in Figure 5. It can be seen that activated carbon has the highest retentive capacity among the four materials studied. This was expected since it has the highest pore volume per unit weight of material (0.8 cc/b). Silica gel and molecular sieve have about the same retentive capacity. The pore volume of silica gel ranged from 0.39 to 0.45 cc/g, while that of molecular sieve is calculated to be 0.22 cc/g. Silica is a nonporous material. Its retentive capacity is expected to be the lowest. It is interesting to note that the retention number for activated carbon-water was higher than 1.00. This indicated that water penetrated into the micropores of the activated carbon particles even though water does not wet activated carbon completely (contact angle = 66°, ref. 2).

Table 3

INTERCEPTS AND SLOPE CONSTANTS

Horizontal Capillary Penetration Through Porous Beds of
Random-Packed Particles.

| <u>Solid</u> | <u>Particle Size Mesh</u> | <u>Porosity %</u> | <u>a</u> | <u>b</u> |
|-------------------------------|-------------------------------|-----------------------|-------------------|----------|
| Activated Carbon | (-40 + 50) to (-180 + 200) | 34.0-45.6 | 4.7×10^6 | 0.61 |
| Silica Gel | (-80 + 100) to (-100 + 200) | 31.0-41.5 | 2.8×10^6 | 0.59 |
| Molecular Sieve | -40 + 60 | 52.8-57.4 | 7.5×10^6 | 0.55 |
| Silica | (-40 + 60) to (-140 + 180) | 34.5-47.9 | 1.3×10^6 | 0.51 |
| Glass Beads (acid cleaned) | -60 + 100 | 29.5-34.7 | 8.8×10^5 | 0.56 |

$$\left[\frac{D_p^2 \gamma_L \cos \theta g_c \rho X}{L \mu^2 (1-X)^2} \right] = a \left[\frac{D_p^2 \rho}{t \mu} \right]^b$$

17

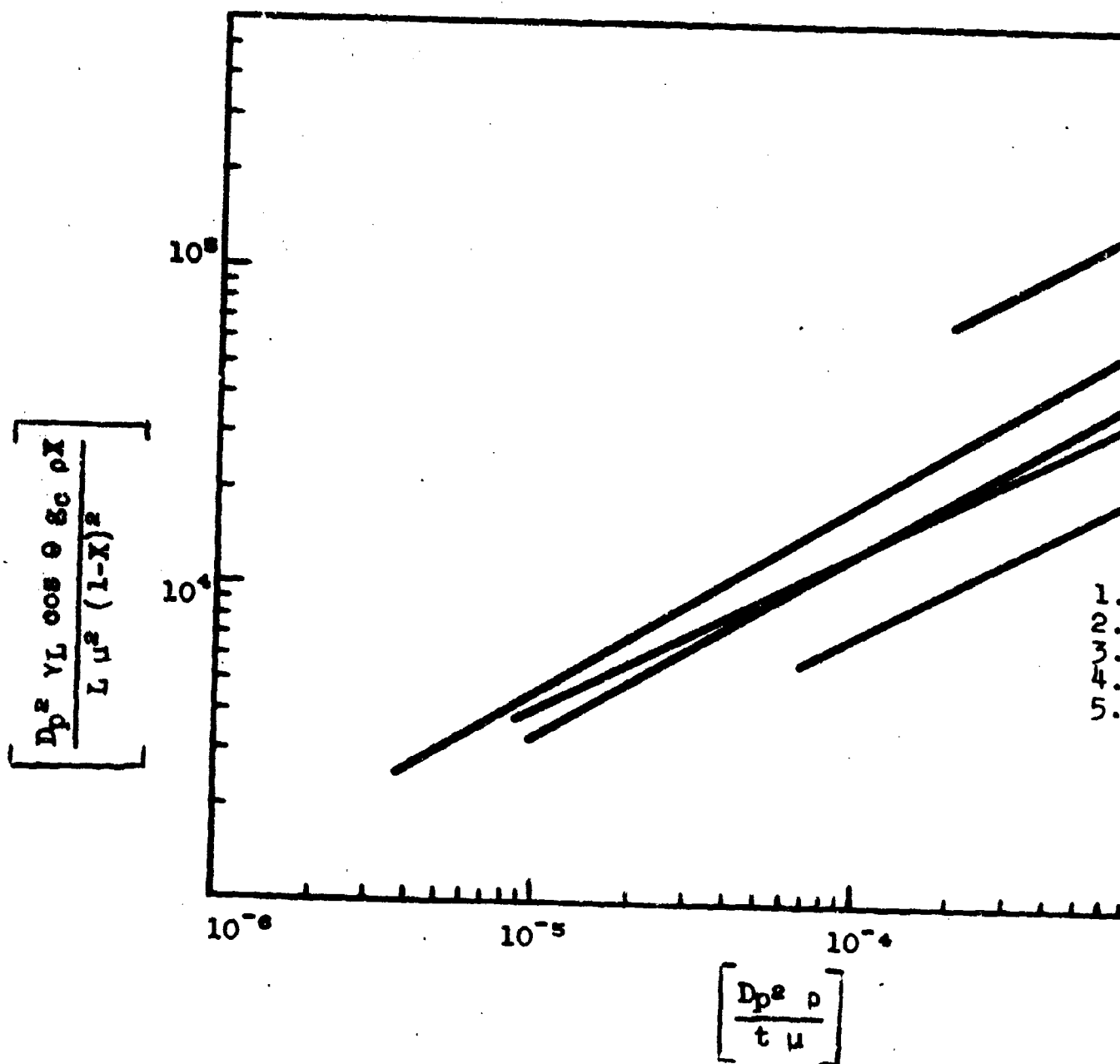
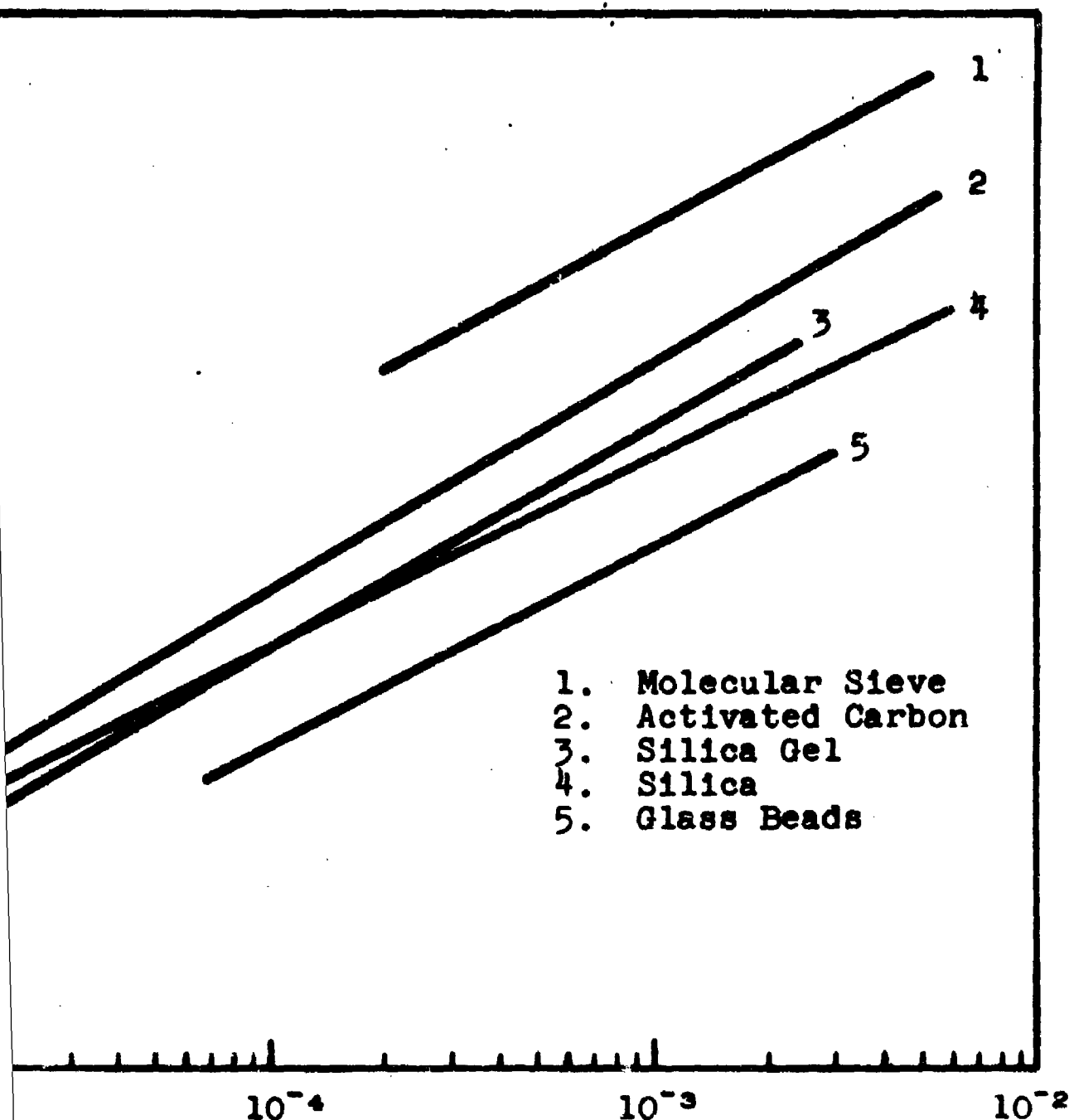


Figure 4. Correlation of Experimental Data on Horizontal Penetration of Liquids Through Random-Packs



$$\left[\frac{D_p^2 \rho}{t \mu} \right]$$

Experimental Data on Horizontal Capillary
Liquids Through Random-Packed Porous Beds.

Table 4

RETENTIVE CAPACITIES OF SOME SOLID SORBENTS

$$\text{Capillary Number} = \frac{D_p^2 \rho g X}{V_L \cos \theta (1-X)^2}$$

$$\text{Retention Number} = \frac{V_L}{V_{BX}}$$

18

| <u>Solid</u> | <u>Liquid</u> | <u>Particle Size mesh</u> | <u>Porosity %</u> | <u>Capilla Numbe</u> |
|------------------|---------------|-------------------------------|-----------------------|--------------------------|
| Activated Carbon | Benzene | -40 + 50 | 40.2 | 4.32 x |
| " " | " | -40 + 50 | 41.5 | 4.65 x |
| " " | " | -40 + 50 | 40.6 | 4.41 x |
| " " | " | -80 + 100 | 39.8 | 8.60 x |
| " " | " | -140 + 180 | 41.5 | 2.02 x |
| " " | Acetone | -80 + 100 | 41.1 | 1.02 x |
| " " | " | -200 + 300 | 37.9 | 1.21 x |
| " " | Water | -80 + 100 | 43.9 | 1.21 x |
| " " | " | -200 + 300 | 38.9 | 1.30 x |
| Silica Gel | Benzene | -40 + 50 | 51.0 | 8.10 x |
| " " | " | -100 + 200 | 46.2 | 5.90 x |
| Molecular Sieve | " | -20 + 40 | 57.9 | 3.84 x |
| " " | " | -40 + 60 | 58.4 | 1.12 x |
| Silica | Benzene | -40 + 60 | 39.0 | 3.48 x |
| " " | " | -200 + 300 | 51.0 | 2.44 x |
| " " | " | -200 + 300 | 48.3 | 2.05 x |

Table 4

CAPACITIES OF SOME SOLID SORBENTS

$$\text{Number} = \left[\frac{D_p^2 \rho g X}{\gamma_L \cos \theta (1-X)^2} \right]$$

$$\text{Number} = \left[\frac{V_L}{V_{BX}} \right]$$

| Particle Size mesh | Porosity % | Capillary Number | Retention Number |
|-----------------------|---------------|-----------------------|---------------------|
| -40 + 50 | 40.2 | 4.32×10^{-2} | 1.50 |
| -40 + 50 | 41.5 | 4.65×10^{-2} | 1.29 |
| -40 + 50 | 40.6 | 4.41×10^{-2} | 1.34 |
| -80 + 100 | 39.8 | 8.60×10^{-3} | 1.88 |
| -140 + 180 | 41.5 | 2.02×10^{-3} | 2.27 |
| -80 + 100 | 41.1 | 1.02×10^{-2} | 1.85 |
| -200 + 300 | 37.9 | 1.21×10^{-3} | 2.15 |
| -80 + 100 | 43.9 | 1.21×10^{-2} | 1.47 |
| -200 + 300 | 38.9 | 1.30×10^{-3} | 1.91 |
| -40 + 50 | 51.0 | 8.10×10^{-2} | 0.91 |
| -100 + 200 | 46.2 | 5.90×10^{-3} | 1.38 |
| -20 + 40 | 57.9 | 3.84×10^{-1} | 0.81 |
| -40 + 60 | 58.4 | 1.12×10^{-1} | 0.91 |
| -40 + 60 | 39.0 | 3.48×10^{-2} | 0.38 |
| -200 + 300 | 51.0 | 2.44×10^{-3} | 0.89 |
| -200 + 300 | 48.3 | 2.05×10^{-3} | 1.00 |

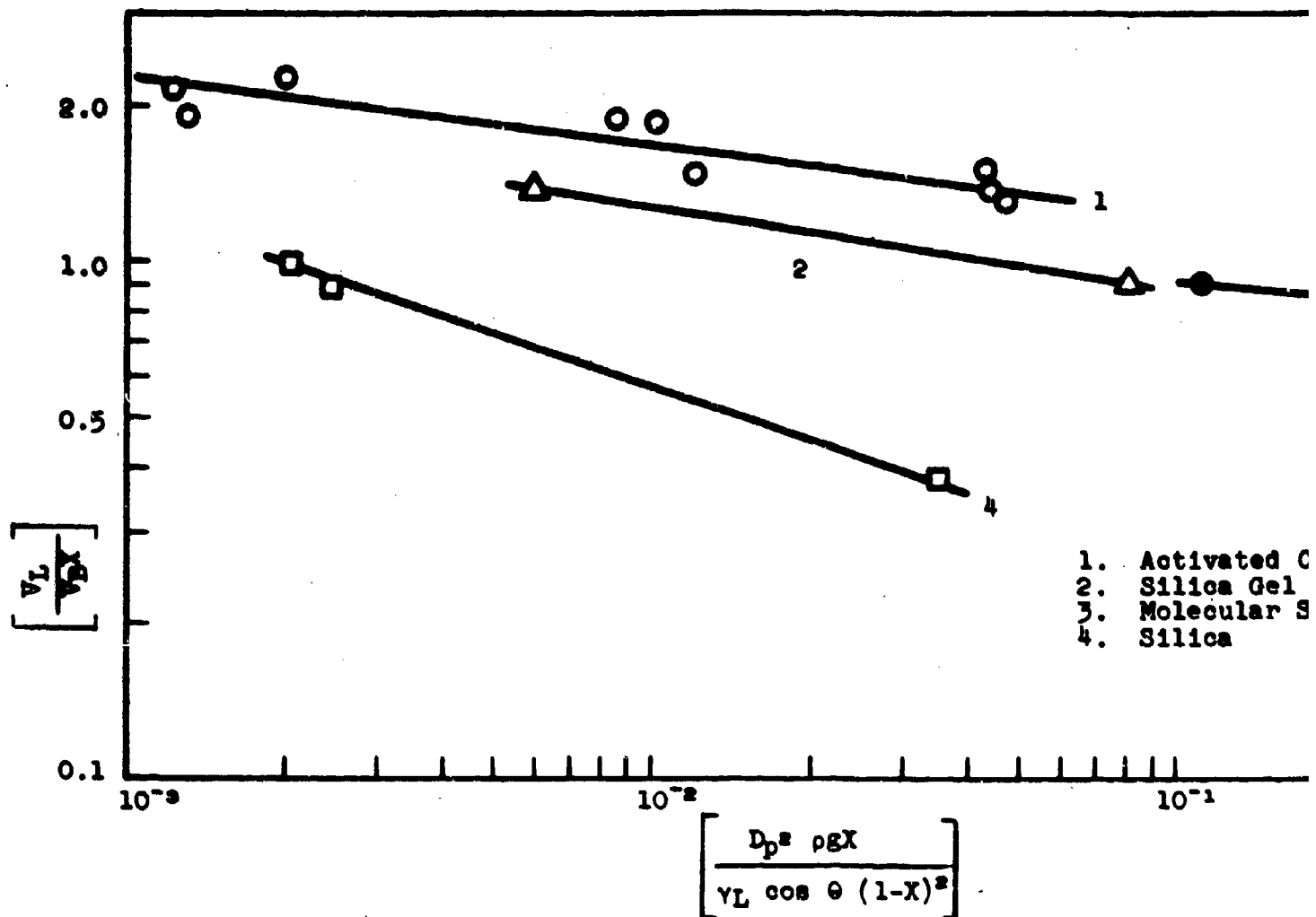
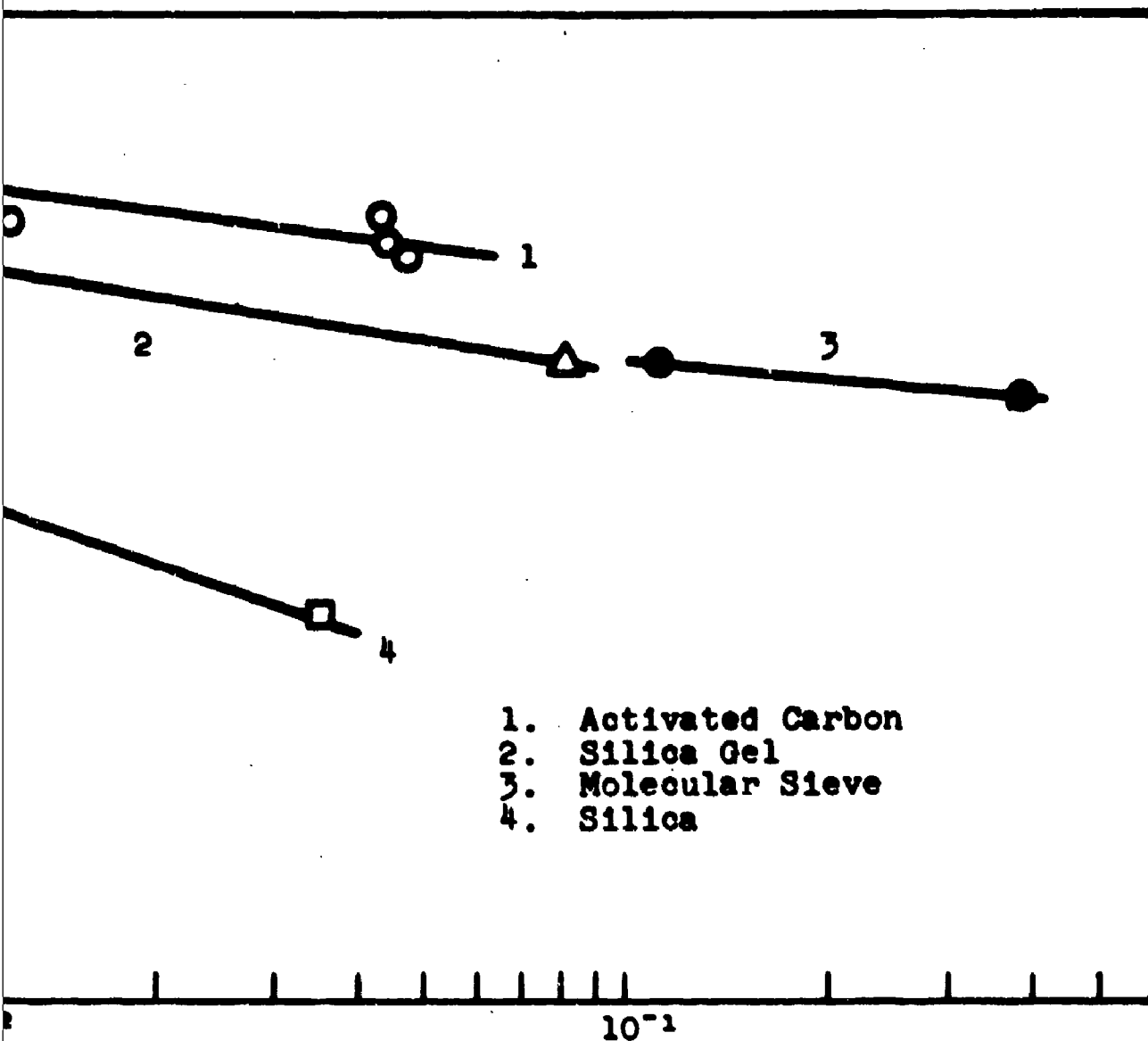


Figure 5. Correlation of Experimental Data on Retentive Capacity of Random Porous Beds.



$$\left[\frac{D_p^2 \rho g X}{\gamma_L \cos \theta (1-X)^2} \right]$$

Experimental Data on Retentive Capacity of Random-Packed

C. CORRELATION OF CAPILLARY PENETRATION AND RETENTIVE CAPACITY

In the capillary penetration experiment, the depth of penetration of the liquid into the porous bed is measured as a function of time. If the solid is a nonporous material, such as silica and glass beads, the amount of material penetrating into the bed will be proportional to the depth of penetration for a given porosity. However, this will not be true if the solid itself is a porous material because the liquid will go into the micropores within particles as well as into the interstitial voids between particles. Since all practical sorbents, such as activated carbon, silica gel and molecular sieve, are porous solids, the actual amount of liquid absorbed by the bed at a given time cannot be measured by the depth of penetration alone. It also depends on the micropore volume and the characteristics of the bed.

To estimate the actual amount of liquid that can be removed by the bed (that is, be retained by the bed) at a given time, the data on capillary penetration were correlated with those on retentive capacity.

The retentive capacity of a solid is measured by the volume of liquid retained, V_L , per unit volume of interstitial void, V_{BX} . Noting that the volume of the bed, V_B , is equal to the length of the bed, L , times the cross-sectional area, A , equation (12) can be expressed as:

$$\left[\frac{V_L}{V_{BX}} \right] = \left[\frac{V_L}{ALX} \right] = m \left[\frac{D_p^2 \rho g X}{V_L \cos \theta (1-X)^2} \right]^n \quad (13)$$

where m and n are constants for a given sorbent.

In the process of capillary penetration, the depth of penetration at a given time is the length of the sorbent bed at that time. Eliminating the variable L from equations (11) and (13), the volume of liquid that can be removed by the bed can be related to the contact time, t :

$$\left[\frac{m g_0 D_p^{2n+2} \rho^{n+1} g^n X^{n+2}}{V_L \mu^2 (V_L \cos \theta)^{n-1} (1-X)^{2n+2}} \right] = a \left[\frac{D_p^2 \rho}{t \mu} \right]^b \quad (14)$$

where $V_L = \frac{V_L}{A}$ = volume of liquid retained per unit exposed area.

The depth of penetration, L , and the volume of liquid retained per unit exposed area, V_L , for four different solids are given in Table 5 as a function of time. The depth of penetration versus time is shown in Figure 6, and the volume of liquid retained versus time is shown in Figure 7. These figures show that silica gave the highest rate of penetration for benzene but the volume of benzene retained by the bed was much lower than that retained by activated carbon and silica gel.

Table 5

DEPTH OF CAPILLARY PENETRATION OF BENZENE AND THE
VOLUME RETAINED BY RANDOM-PACKED POROUS BEDS

| Time sec | Activated Carbon | | Silica Gel | | Molecular Sieve | | Silica | |
|-------------|---------------------|-----------------------------|---------------|-----------------------------|--------------------|-----------------------------|---------|-----------------------------|
| | L cm | V_L cc/cm ² | L cm | V_L cc/cm ² | L cm | V_L cc/cm ² | L cm | V_L cc/cm ² |
| 1 | 0.56 | 0.31 | 0.91 | 0.36 | 0.32 | 0.13 | 1.68 | 0.23 |
| 2 | 0.87 | 0.48 | 1.34 | 0.54 | 0.48 | 0.19 | 2.38 | 0.33 |
| 3 | 1.08 | 0.60 | 1.73 | 0.69 | 0.58 | 0.23 | 2.88 | 0.40 |
| 4 | 1.27 | 0.70 | 2.02 | 0.81 | 0.68 | 0.27 | 3.34 | 0.47 |
| 5 | 1.46 | 0.81 | 2.32 | 0.93 | 0.77 | 0.30 | 3.74 | 0.52 |
| 6 | 1.64 | 0.91 | 2.57 | 1.03 | 0.86 | 0.34 | 4.06 | 0.57 |
| 7 | 1.79 | 0.99 | 2.80 | 1.12 | 0.93 | 0.36 | 4.38 | 0.62 |
| 8 | 1.94 | 1.07 | 3.02 | 1.21 | 1.00 | 0.39 | 4.75 | 0.66 |
| 9 | 2.11 | 1.16 | 3.22 | 1.29 | 1.06 | 0.42 | 5.00 | 0.70 |
| 10 | 2.21 | 1.22 | 3.39 | 1.36 | 1.10 | 0.43 | 5.28 | 0.74 |

L = Depth of capillary penetration

V_L = Volume of liquid retained per unit exposed area

Temperature = 25°C

Porosity = 40%

Particle Size = -40+50 mesh

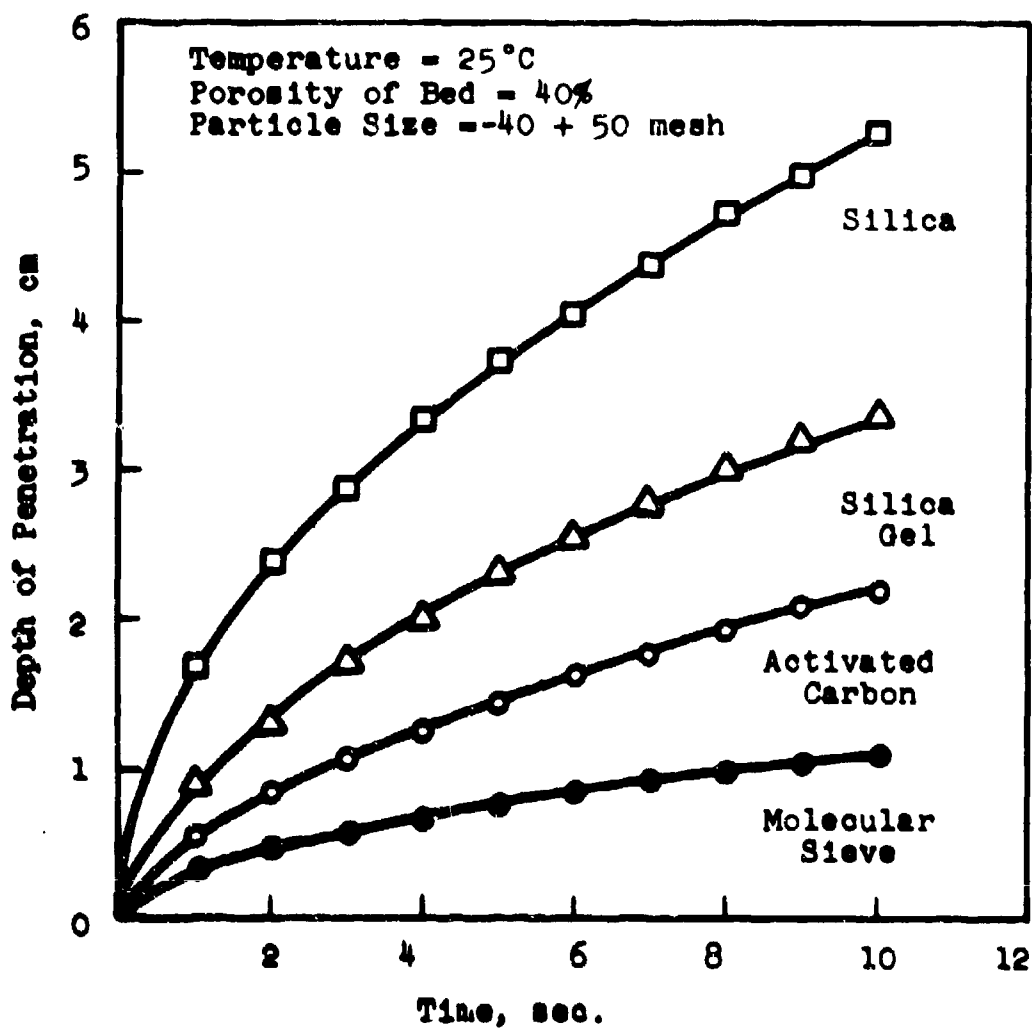


Figure 6. Depth of Horizontal Capillary Penetration of Benzene Through Random-Packed Porous Beds.

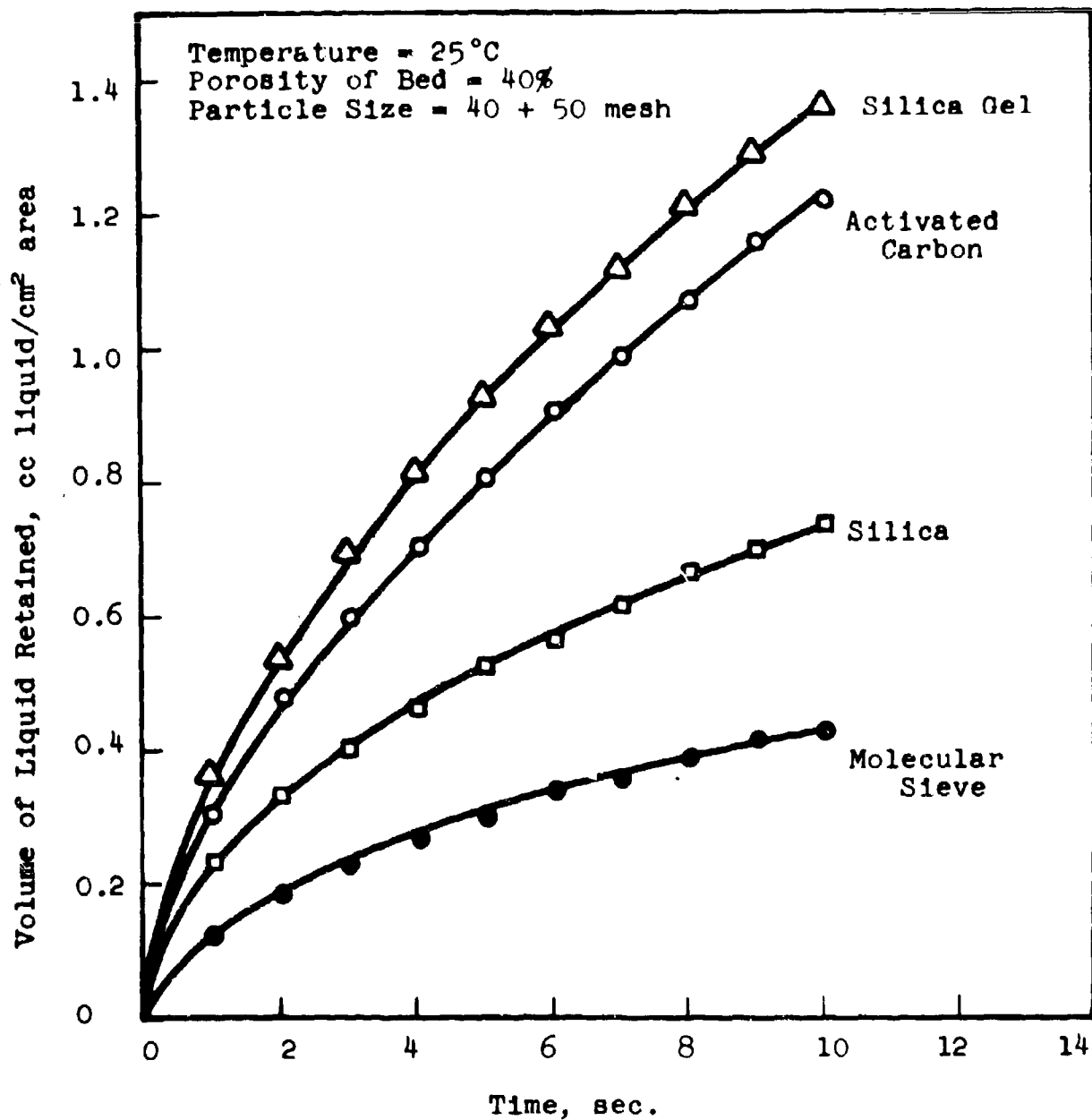


Figure 7. Volume of Benzene Retained by Random-Packed Porous Beds As a Function of Contact Time.

Judging from the results obtained, silica gel seems to remove benzene most rapidly but activated carbon has the highest retentive capacity.

D. MEASUREMENTS ON CHEMICAL WARFARE AGENTS

Actual measurements on liquid phase sorption of chemical warfare agents are being made. The results will be presented in the next progress report.

IV. REFERENCES

1. Smith, J. O., Fabuss, B. M., Duncan, D. A., Lu, C. H., "Third Bimonthly Progress Report", Contract DA-18-108-AMC-238(A), 18 February 1964.
2. Smith, J. O., Fabuss, B. M., Duncan, D. A., Lu, C. H., "Fourth Bimonthly Progress Report", Contract DA-18-108-AMC-238(A), 16 April 1964.
3. Brown, G. G. and Associates, "Unit Operations", pp. 211-214, John Wiley and Sons, Inc., New York, 1950.
4. Kirk, R. E. and Othmer, D. F., "Encyclopedia of Chemical Technology", Vol. 12, p. 347, The Interscience Encyclopedia, Inc., New York, 1954.